

Chapter 25

Preparation of Random and Aligned Polycaprolactone Fiber as Template for Classical Calcium Oxalate Through Electrocrystallization



Lazy Farias, Nicole Butto, and Andrónico Neira-Carrillo

Abstract The aim of this study was to evaluate the effect of random and oriented electrospun polycaprolactone (PCL) fiber meshes on conductive indium tin oxide (ITO) electrode on the in vitro electrocrystallization (EC) of calcium oxalate (CaOx). For that, random and aligned PCL fibers were prepared through flat and rotating collectors and directly collected on conductive ITO support that was used as organic solid template for controlling the in vitro EC of CaOx. Our findings revealed that electrospun PCL surface topology induced preferentially the nucleation and crystal growth of CaOx along on individual aligned PCL fibers during the EC of CaOx. Scanning electron microscopy (SEM), energy dispersive X-ray spectroscopy (EDX), chronoamperometry, and X-ray diffraction (XRD) spectroscopy of CaOx crystals show that the morphological orientation of PCL fiber meshes acted as selective good nucleation site at PCL surface controlling their CaOx crystal morphologies and the crystallographic orientation of crystals inducing the coexistence of dehydrated CaOx (COD) and monohydrated CaOx (COM) crystals as the unique polymorphism.

Keywords Electrospun fibers · Electrocrystallization · Calcium oxalate (CaOx) · Indium zinc oxide (ITO) · Polycaprolactone (PCL) · Dehydrated CaOx (COD) · Monohydrated CaOx (COM)

L. Farias · N. Butto · A. Neira-Carrillo (✉)
Department of Biological and Animal Sciences, School of Veterinary and Animal Sciences,
University of Chile, Santiago, Chile
e-mail: nbutto@veterinaria.uchile.cl; aneira@uchile.cl

25.1 Introduction

Biological crystallization or biomineralization is the process by which living organisms from bacteria to eukaryotes cells form hierarchical hybrid biogenic minerals (Lowenstam and Weiner 1989; Estroff 2008). Its role in nature is diverse such as protection, motion, storage, optical and gravity sensing, defense, detoxification, etc. (Mann 2000). They are highly organized from molecular level to the nano- and macroscale, with intricate nano-architectures that ultimately make up a myriad and remarkable properties and complex shape of different functional soft and hard tissues (Sumper and Brunner 2006; Guru and Dash 2014; Neira-Carrillo et al. 2015a, b). These properties can inspire mimetic strategies intending to design nanomaterials based on mineral controlled crystallization concept. Biological crystallization, however, also occurs in a pathological manner in nature, e.g., concretions, gallstones (Wang et al. 2006; Xie et al. 2015), and the mineralization of CaOx within the urinary tract often called urolithiasis (Khan and Canales 2009). Therefore, biominerals are outstanding materials not only for understanding the biomineralization concept but also for novel confined-materials synthesis and design, avoiding undesirable pathological biomineralization. Composite biogenic nanomaterials are also of increasing interest to materials scientists who seek novel materials syntheses such as fibrillary hydrogel, platelet or fiber structures, and crystalline matrices and/or interfaces with similar crystalline forms to those produced by nature. There is an abundant diversity of chemical compositions and structures for minerals such as carbonates, silicates, phosphates, oxalate, oxides, etc. (Pai and Pillai 2008; Neira-Carrillo et al. 2010, 2015a, b). In general, *in vitro* study of inorganic minerals can be performed by using additives or organic substrates through different experimental methodologies.

With this in mind, random and oriented electrospun polycaprolactone (PCL) fiber meshes on indium tin oxide (ITO) support were prepared through electrospinning and used as an organic template for controlling the *in vitro* electrocrystallization (EC) of CaOx. Electrospinning is a nanofabrication technique, in which the organic polymer fibers orientation can be topologically controlled at the surface of PCL meshes. Electrospinning involves the application of an electric field to a drop of polymer solution that is deformed and forced to be ejected to a metallic plate collector in which the arrangement of fibers can be controlled with random (Kishan and Cosgriff-Hernandez 2017) or aligned (Lee et al. 2017) fibers orientation.

Therefore, in order to study the effect of PCL surface topology as organic solid template for controlling the *in vitro* EC of CaOx, random and aligned PCL fibers were directly collected on ITO glass electrode by using flat and rotating collectors. The use of EC has been documented for CaOx (Neira-Carrillo et al. 2015a, b) and for other inorganic minerals such as calcium carbonate crystals (Pavez et al. 2004; Buttlo et al. 2017; Sanchez et al. 2017).

25.2 Materials and Methods

The *in vitro* EC of CaOx on PCL electrospun fiber meshes was carried out onto conductive ITO electrode at 9 mA using 18% PCL solution (Mw, 80,000, Sigma-Aldrich) in organic ethyl acetone/acetate 3:1 (v:v) solvents in an electrospinning instrument (Fluidnatek® LE-10). Random and aligned PCL fiber meshes were spun on a fixed metal flat (30 × 30 cm) and rotary (10 cm in diameter) collectors, respectively. The control of PCL surface topology was achieved by using the following parameters: 16 kV, solution flow rate of 1200 $\mu\text{l/h}$, 15 min, nozzle-collector distance from between 15 and 18 cm, and rotating speed of 2000 rpm. The modified ITO-containing PCL fiber meshes were immersed in an electrocrystallization solution composed of sodium oxalate (Sigma-Aldrich®), calcium nitrate (MERCK®), and ethylenediaminetetraacetic acid tetrasodium salt (Sigma-Aldrich®) and put into an electrochemical cell. The potentiostat-galvanostat (Epsilon-BASi) instrument and the Epsilon EC-USB program were used for performing all the EC of CaOx assays. The SEM-EDX surface morphology of the resultant CaOx crystals was examined using a scanning electron microscope (Jeol JSM-IT300LV, JEOL USA Inc., USA) connected to an energy dispersive X-ray detector for elemental analysis with computer-controlled software, the Aztec EDX system (Oxford Instruments, Abingdon, UK). Powder X-ray diffraction (PXRD) was performed by using a Siemens D-5000X X-ray diffractometer with Cu-K α radiation (graphite monochromator) and an ENRAF Nonius FR 590. The crystal structure of CaOx was determined by using Cu-K α radiation (40 kV), steps of 0.2°, and the geometric Bragg-Brentano (θ - θ) scanning mode with an angle (2θ) range of 5–70°. The DiffracPlus program was used as a data control software.

25.3 Results

25.3.1 *Preparation of PCL Fibers and Chronopotentiometric Curve of CaOx*

Random and oriented electrospun polycaprolactone (PCL) fiber meshes were prepared by using electrospinning directly deposited on ITO support as working electrode for conducting the *in vitro* EC of CaOx. Therefore, EC of CaOx using surface-modified ITO PCL fiber meshes with controlled topology was used as solid template, and their electrochemical potentiometric behavior follows at room temperature for 5 min. We observed a notorious difference in the behavior of electrochemical curves during the EC of CaOx when both surface-modified ITO PCL fiber meshes were used indicating a different mechanism of CaOx crystallization

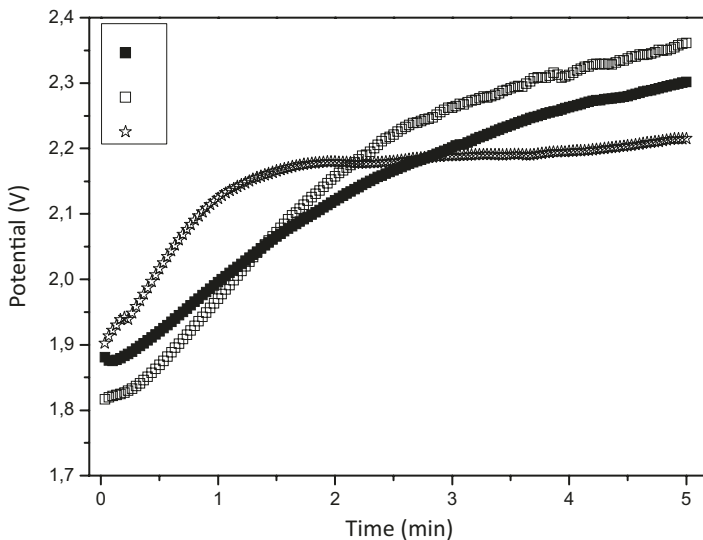


Fig. 25.1 Chronopotentiometric curves for EC of CaOx crystals on ITO electrode substrate. Without additive as control (■) and in the presence of random PCL fiber (□) and aligned PCL fiber (☆) meshes

(Fig. 25.1). This can be rationalized by increasing the formed CaOx material when the EC was performed at constant applied current of 9 mA. Thus, when the in vitro EC of CaOx in the presence of aligned PCL fiber mesh was performed (Fig. 25.1 ☆), the electrochemical potential reached a maximum value of 2.2 V at 1.5 min, keeping this constant value until the end of the test. Meanwhile when the PCL fiber meshes with random distribution were used as template (Fig. 25.1 □), the potential (V) showed a progressive increase behavior of 2.35 V until the end of the experiment. The same potentiometric curve was also observed in absence of surface-modified ITO as control essays reaching ca. of 2.30 V until the end of the experiment.

25.3.2 SEM, EDX, and XRD Characterization of CaOx Obtained by EC Method

The morphological aspect and distribution of CaOx crystals grown on modified-ITO support were carried out by scanning electron microscopy (SEM). SEM analysis showed that crystals grown on surface-modified ITO with randomly PCL fibers were found into network-PCL fiber mesh forming conglomerate crystalline particles. Here, classic bipyramidal morphology of COD crystals was observed (Fig. 25.2a). On the other hand, CaOx crystals formed on surface-modified ITO with aligned PCL fibers grown along and surrounding on PCL fibers (inset, Fig. 25.2b). Here, we also observed several COD crystals with distinct

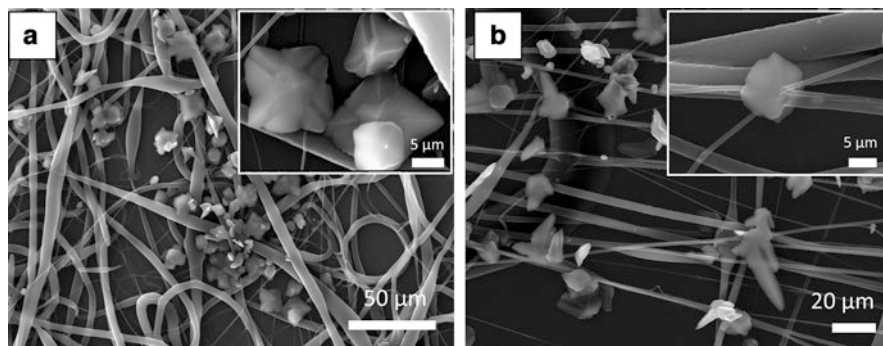


Fig. 25.2 SEM images of CaOx crystals obtained through EC method on surface-modified ITO with (a) random PCL fiber and (b) with aligned PCL fibers meshes

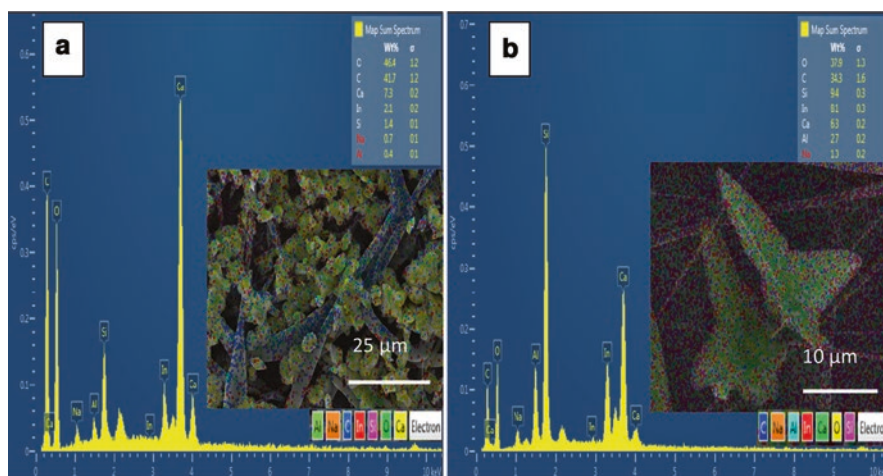


Fig. 25.3 EDX measurements of CaOx crystals obtained through EC method on surface-modified ITO with (a) random PCL fiber and (b) aligned PCL fiber meshes. The colors assigned to each element were arbitrarily selected in the EDX measurements

morphological COD with slight crystalline shape of CaOx crystals (Fig. 25.2b). Regular and flower-like COD crystals morphologies were also observed in other part deposited on aligned PCL fiber samples. This result indicated that the growth of crystal faces normal to the [100] direction was selectively inhibited by changing the topological surface of PCL fibers as template on the surface-modified ITO support.

The energy dispersive X-ray spectroscopy (EDX) detector on CaOx crystals was also used, demonstrating the characteristic elemental and chemical composition of CaOx crystals (Fig. 25.3) and to the conductive ITO support. The SEM and EDX studies of CaOx were carried out by using “analysis” as observation condition and the “charge-up reduction mode” as observation mode. The weight percent (wt.-%) concentration of elements at the crystal surface was automatically calculated

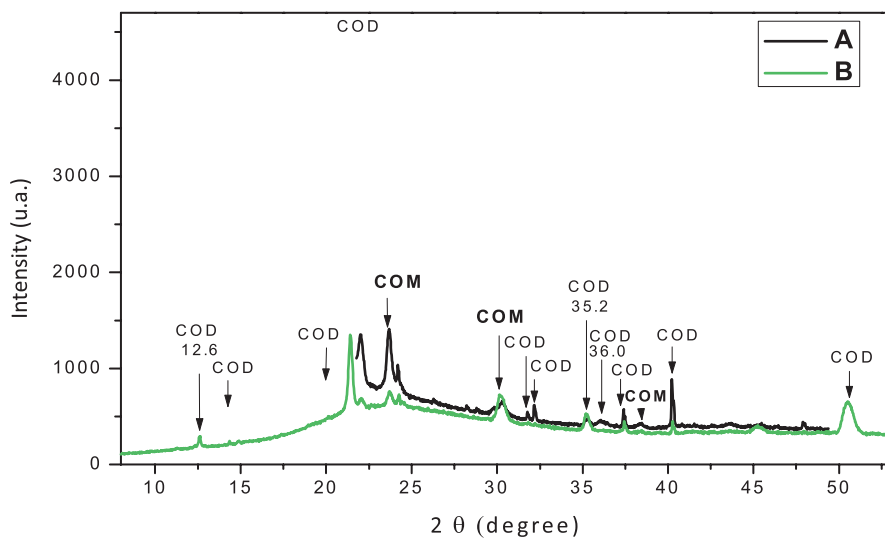


Fig. 25.4 XRD spectra of CaOx crystals obtained through EC on surface-modified ITO with (a) random PCL fibers mesh, black line, and (b) aligned PCL fibers mesh, green line. Diffraction peaks show crystalline polymorphs of monohydrate (COM) and dihydrate (COD) CaOx

through EDX software. In order to determine the internal lattice of crystalline CaOx products, X-ray diffraction (XRD) analysis was also performed. Figure 25.4 shows XRD pattern of CaOx crystals obtained by EC in the presence of surface-modified ITO with random PCL fibers (Fig. 25.4a) and surface-modified ITO with aligned PCL fibers (Fig. 25.4b). In general, the XRD spectra demonstrated the coexistence of COD and COM polymorphism; the crystalline peaks showed slight difference in the intensity of the main reflections of COD and COM, which are ascribed at $2\theta = 14.3^\circ, 20.0^\circ, 21.3^\circ, 32.2^\circ, 37.2^\circ, 40.2^\circ,$ and 50.7° and $2\theta = 15.0^\circ, 23.0^\circ, 67.0^\circ,$ and 30.2° , respectively. It was noted that the portion of COD crystals in the resultant product on surface-modified ITO became dominant. The current type of CaOx polymorphism designations is in agreement with COM and COD crystals obtained by using acid-rich biopolymers as additive (Jung et al. 2005).

25.4 Discussion

In vitro electrocrystallization on controlled surface-modified ITO with PCL fiber meshes as classical crystallization of CaOx was performed. Thus, EC of CaOx on ITO working electrode with random and aligned electrospun PCL fibers was used as solid template to evaluate the topology effect onto ITO electrode on the morphology, distribution, and polymorphism of the CaOx crystals. Random and aligned

PCL fibers were obtained by using flat and rotary collectors through electrospinning technique, respectively. In summary, CaOx crystals were effectively electrodeposited, and a clear difference in the distribution, morphology, and crystal growth of CaOx crystals was observed. We suggest that the active surface topology of PCL fiber meshes can act as good nucleation point and in particular on the aligned surface of each PCL fibers inducing a favorable site for the *in vitro* crystallization of CaOx. In addition, polymorphism of CaOx can be selectively controlled onto surface-modified ITO, although the absence of chemical functionality on PCL fiber as template. Here, we observed a coexistence in the polymorphism of calcium oxalate; however, the COD crystals were the predominant particles on the surface of the ITO substrates.

Acknowledgments The authors are grateful to Project Fondecyt 1171520 and 1140660, Program U-Redes, Vice-Presidency of Research and Development, University of Chile.

References

- Buttlo N, Cabrerías-Barjas G, Neira-Carrillo A (2017) Electrocrystallization of CaCO₃ crystals obtained through phosphorylated chitin. Crystals. Submitted_ID: Crystals-260718
- Estroff LA (2008) Introduction: on biomineralization. *Chem Rev* 108:4329–4331
- Guru PS, Dash S (2014) Sorption on eggshell waste—a review on ultrastructure, biomineralization and other applications. *Adv Colloid Interf Sci* 209:49–67
- Jung T, Kim WS, Choi CK (2005) Crystal structure and morphology control of calcium oxalate using biopolymeric additives in crystallization. *J Cryst Growth* 279:154–162
- Khan S, Canales B (2009) Genetic basis of renal cellular dysfunction and the formation of kidney stones. *Urol Res* 37:169–180
- Kishan AP, Cosgriff-Hernandez EM (2017) Recent advancements in electrospinning design for tissue engineering applications: a review. *J Biomed Mater Res A* 105:2892–2905
- Lee SJ, Heo M, Lee D, Heo DN, Lim HN, Kwon IK (2017) Fabrication and design of bioactive agent coated, highly-aligned electrospun matrices for nerve tissue engineering: preparation, characterization and application. *Appl Surf Sci* 424:359–367
- Lowenstam HA, Weiner S (1989) *On biomineralization*. Oxford University Press, New York
- Mann S (2000) The chemistry of form. *Angew Chem Int Ed* 39:3392–3406
- Neira-Carrillo A, Yazdani-Pedram P, Vasquez-Quitral P, Arias JL (2010) Selective calcium oxalate crystallization induced by monomethylitaconate grafted polymethylsiloxane. *Mol Cryst Liq Cryst* 522:307–317
- Neira-Carrillo A, Vásquez-Quitral P, Fernández MS, Luengo-Ponce F, Yazdani-Pedram M, Cölfen H, Arias JL (2015a) Sulfonated polymethylsiloxane as an additive for selective calcium oxalate crystallization. *Eur J Inorg Chem* 2015(7):1167–1177
- Neira-Carrillo A, Vásquez-Quitral P, Sánchez M, Vargas-Fernández A, Silva F (2015b) Control of calcium oxalate morphology through electrocrystallization as an electrochemical approach for preventing pathological disease. *Ionics* 21:3141–3149
- Pai R, Pillai S (2008) Divalent cation-induced variations in polyelectrolyte conformation and controlling calcite morphologies: direct observation of the phase transition by atomic force microscopy. *J Am Chem Soc* 130:13074–13078
- Pavez J, Silva J, Melo F (2004) Homogeneous calcium carbonate coating obtained by electrodeposition: *in situ* atomic force microscope observations. *Electrochim Acta* 50:3488–3494

- Sánchez M, Vásquez-Quitral P, Butto N, Díaz-Soler F, Yazdani-Pedram M, Silva JF, Neira-Carrillo A (2017) Effect of alginate from Chilean *Lessonia nigrescens* and MWCNTs on CaCO₃ crystallization by classical and non-classical methods. Crystals, Submitted_ID: Crystals-260775
- Sumper M, Brunner E (2006) Learning from diatoms: nature's tools for the production of nanostructured silica. Adv Funct Mater 16:17–26
- Wang L, Qiu SR, Zachowicz W, Guan XY, DeYoreo JJ, Nancollas GH, Hoyer JR (2006) Modulation of calcium oxalate crystallization by linear aspartic acid-rich peptides. Langmuir 22:7279–7285
- Xie B, Halter TJ, Borah BM, Nancollas GH (2015) Aggregation of calcium phosphate and oxalate phases in the formation of renal stones. Cryst Growth Des 15:204–211

Open Access This chapter is licensed under the terms of the Creative Commons Attribution 4.0 International License (<http://creativecommons.org/licenses/by/4.0/>), which permits use, sharing, adaptation, distribution and reproduction in any medium or format, as long as you give appropriate credit to the original author(s) and the source, provide a link to the Creative Commons license and indicate if changes were made.

The images or other third party material in this chapter are included in the chapter's Creative Commons license, unless indicated otherwise in a credit line to the material. If material is not included in the chapter's Creative Commons license and your intended use is not permitted by statutory regulation or exceeds the permitted use, you will need to obtain permission directly from the copyright holder.

